文章编号：1001-9014(2024)06-0828-05

DOI:10.11972/j.issn.1001-9014.2024.06.014

High polarization extinction ratio achieved base on thin-film lithium niobate

YANG Yong-Kang[1,2], GUO Hong-Jie[1,2], CHEN Wen-Bin[1,2], QU Bai-Ang[1,2], YU Zhi-Guo[2], TAN Man-Qing[1,2*], GUO Wen-Tao[1,2*], LIU Hai-Feng[3]

(1. University of Chinese Academy of Sciences, Beijing 100049, China;
2. Key Laboratory of Optoelectronics Materials and Devices, Institute of Semiconductors, Chinese Academy of Sciences, Beijing 100083, China;
3. Beijing Huairou Instruments and Sensors Co, Ltd, Beijing 101400, China)

Abstract: This article introduces a method of achieving high polarization extinction ratio using a subwavelength grating structure on a lithium niobate thin film platform, and the chip is formed on the surface of the lithium niobate thin film. The chip, with a length of just 20 μm, achieved a measured polarization extinction ratio of 29 dB at 1 550 nm wavelength. This progress not only proves the possibility of achieving a high extinction ratio on a lithium niobate thin film platform, but also offers important technical references for future work on polarization beam splitters, integrated fiber optic gyroscopes, and soon.

Key words: Lithium niobate, thin film lithium niobate, subwavelength grating, polarization extinction ratio, photonic integrated circuits

基于薄膜铌酸锂实现高偏振消光比

杨永康[1,2], 郭宏杰[1,2], 陈文彬[1,2], 屈柏昂[1,2], 于治国[2], 谭满清[1,2*], 郭文涛[1,2*], 刘海峰[3]

(1. 中国科学院大学,北京 100049;
2. 中国科学院半导体研究所 光电子材料与器件重点实验室,北京 100083;
3. 北京怀柔仪器和传感器有限公司,北京 101400)

摘要:本文介绍了一种通过在铌酸锂薄膜平台上使用亚波长光栅结构实现高偏振消光比的方法,并在铌酸锂薄膜的表面形成了芯片。该芯片的长度仅为 20 μm,在 1 550 nm 波长下测得的偏振消光比为 29 dB。这一进展不仅证明了在铌酸锂薄膜平台上实现高偏振消光比的可能性,而且为未来在偏振分束器、集成光纤陀螺仪等方面的工作提供了重要的技术参考。

关 键 词:铌酸锂;铌酸锂薄膜;亚波长光栅;偏振消光比;光子集成

中图分类号:TN29　　**文献标识码**:A

Introduction

Lithium niobate ($LiNbO_3$) has garnered acclaim for its exceptional optical and electrical properties, finding extensive use in optical communication, sensing, and computing. The advent of thin film lithium niobate[1] (TFLN) technology has amplified its potential, offering enhanced modal confinement, low-loss light propagation, and high optical nonlinearity, thus marking it as a pivotal platform for next-generation photonic integrated circuits (PICs)[2-4].

Advancements in $LiNbO_3$ etching techniques have enriched the TFLN components landscape, catering to the demands of various photonic applications, including modulators, wavelength converters, and multiplexers[2]. The intrinsic birefringence of TFLN makes it particularly suited for polarization handling devices, where the capability to selectively transmit transverse electric (TE) or transverse magnetic[5] (TM) polarization modes—quanti-

Received date: 2024-03-22, **revised date**: 2024-05-10　　**收稿日期**:2024-03-22,**修回日期**:2024-05-10

Foundation items: Supported by Beijing Natural Science Foundation (4242062) and the Youth Innovation Promotion Association, CAS (2021108).

Biography: YANG Yong-Kang (1994-), male, Tianshui, Ph. D student. Research area involves semiconductor laser and light source. E-mail: ykyang@semi.ac.cn

* **Corresponding authors**: E-mail: wtguo@semi.ac.cn; mqtan@semi.ac.cn

fied by the polarization extinction ratio (PER)—is critical[1, 4, 6].

Despite the promising attributes of TFLN, achieving high PER is challenging due to nonlinear optical effects, optical absorption, and dispersion during the fabrication process[7]. Strategies like hybrid plasmonic waveguides, highly doped silicon waveguides, epsilon-near-zero materials[6, 8], and notably subwavelength gratings[2] (SWGs) have been explored to overcome these challenges. SWGs, with their compact structure and high extinction ratio efficiency, have emerged as a key solution for developing high-performance, space-efficient photonic devices[2, 9].

In this work, we introduce a novel design of SWG structures on lithium niobate thin films that attains a high PER, evidenced by our experimental results showing a PER of 29 dB at 1550 nm wavelength. This achievement not only sets a new benchmark for $LiNbO_3$ thin film applications but also underscores the potential of compact, efficient SWG designs in advancing the field of integrated photonics, particularly in polarization control and fiber optic gyroscopes[10-12].

1 Principle and Design

1.1 Single Mode

The modulation structure incorporates a ridge waveguide, which is clad with air as shown in Figure 1(a). During the Lithium Niobate on Insulator (LNOI) etching process, we set the sidewall angle to 65° based on references[2, 13]. We evaluated key structural elements like ridge width and ridge height using the Finite Difference Eigenmode (FDE) solver. This tool helps us understand the mode cutoff condition of the ridge waveguide. In Fig. 1(b), it is evident that widening and raising the ridge alter the mode cutoff condition. It changes from supporting only the TE mode (region I) to accommodating both TE and TM modes (region II). Although it's easier to meet TE mode conditions with shallow etching, this approach leads to higher losses. After considering various factors, we chose a ridge width of 0.8 μm and a ridge height of 0.2 μm. These dimensions ensure the ridge waveguide supports only the TE mode, as seen in region I of Fig. 1(b). Consequently, this design ensures the TM mode is cut off, primarily radiating into the Silicon substrate[14].

1.2 Sub-grating

The distinctive feature of Subwavelength Grating[15] (SWG) lies in its periodically arranged blocks that define the metamaterial's optical properties on a large scale. When the grating period is substantially smaller than the wavelength of light, it suppresses diffraction effects. This makes the entire structure appear optically similar to a uniform anisotropic material with an effective dielectric tensor[16]. This principle conceptualizes the waveguide as equivalent to a birefringent crystal. The model of this structure is depicted in Figure 2.

In the given expressions, Λ represents the period of the subwavelength grating structure, n_1 and n_2 are the refractive indices of the materials forming the continuously varying structure, and a corresponds to the length associated with n_1. Incident light on the grating has an electric field polarization that's either parallel or perpendicular to the periodic interface. The corresponding effective refractive indices are calculated using the subsequent equations:

$$n_{\parallel}^2 \approx \frac{a}{\Lambda} n_1^2 + \left(1 - \frac{a}{\Lambda}\right) n_2^2 + O\left(\frac{\Lambda^2}{\lambda^2}\right) \quad , \quad (1)$$

$$n_{\perp}^{-2} \approx \frac{a}{\Lambda} n_1^{-2} + \left(1 - \frac{a}{\Lambda}\right) n_2^{-2} + O\left(\frac{\Lambda^2}{\lambda^2}\right) \quad . \quad (2)$$

The refractive index matrix of the subwavelength grating waveguide, disregarding infinitesimal terms, is:

$$\begin{pmatrix} n_{/\!/} & 0 & 0 \\ 0 & n_{/\!/} & 0 \\ 0 & 0 & n_{\perp} \end{pmatrix} \quad . \quad (3)$$

The formula indicates that by adjusting parameters such as $\frac{a}{\Lambda}$, n_1 and n_2, we can achieve custom birefringence in 'artificial metamaterials'. For practical applications, we can design SWG structures using Bloch's theorem. When the grating has a period Λ, the effective refractive index (n_{eff}) is reflected when $n_{\text{eff}} = \lambda/2\Lambda$, and it can traverse the grating structure with less loss when $n_{\text{eff}} < \lambda/2\Lambda$. During the design process, the fill factor is defined as $n_{\text{eff}} = \lambda/2\Lambda$. Accordingly, n_{eff} is chosen as the fill factor, where $n_{\text{eff}} = a/\Lambda$. For $n_{\text{eff}} = 0.8$, the effective refractive index is determined by scanning various waveguide widths using the mode-FDE module, as demon-

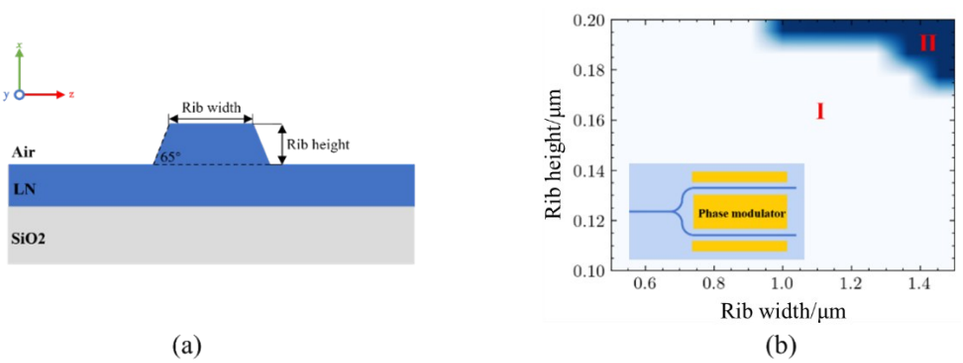

Fig. 1 (a) Ridge waveguide fabrication diagram; (b) ridge waveguide mode diagram
图1 (a)脊型波导制备图和模式图;(b)脊型波导模式图

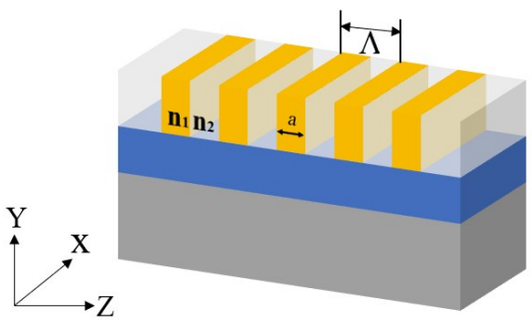

Fig. 2 Subwavelength grating model diagram
图2 亚波长光栅模式图

strated in Figure 3.

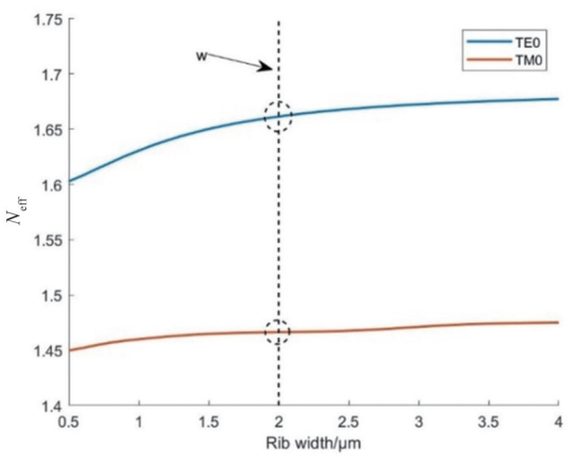

Fig. 3 Effective refractive index plots of TE0 and TM0 under different Rib width
图3 不同脊型宽度下TE0和TM0的有效折射率图

As illustrated in Figure 3, when Rib width of 2 μm, the effective refractive index for the TE0 mode is approximately 1.65, and for the TM0 mode, it is around 1.45. This design strategically enables the TE0 mode to transmit almost entirely while nearly completely blocking the TM0 mode.

Moreover, the subwavelength grating model of lithium niobate nanowaveguides is depicted in Fig. 4. Among them, W_1 denotes the width of the waveguide, W_2 represents the width of the intermediate fishbone waveguide, and W_3 specifies the subwavelength grating's width. Λ signifies the grating period, while L_1, L_2, and L_3 represent the lengths of the transition tapered waveguides. The selected parameters are optimized to achieve ideal results under these specified conditions[17].

The loss plot for the subwavelength grating TEPASS is presented in Fig. 5, demonstrating that the polarization extinction ratio can achieve a remarkable level of up to 34dB. The specific parameters contributing to this performance are detailed in Table 1.

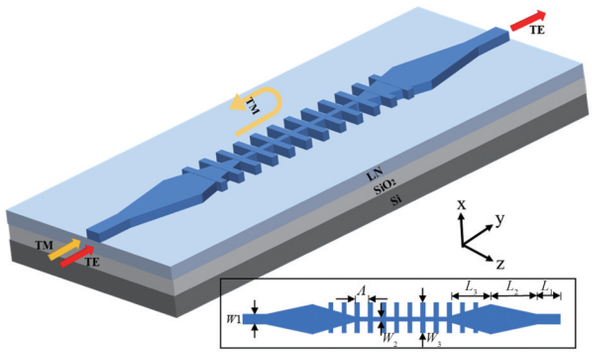

Fig. 4 Lithium niobate nanowaveguide subwavelength grating model diagram
图4 铌酸锂纳米波导亚波长光栅模型图

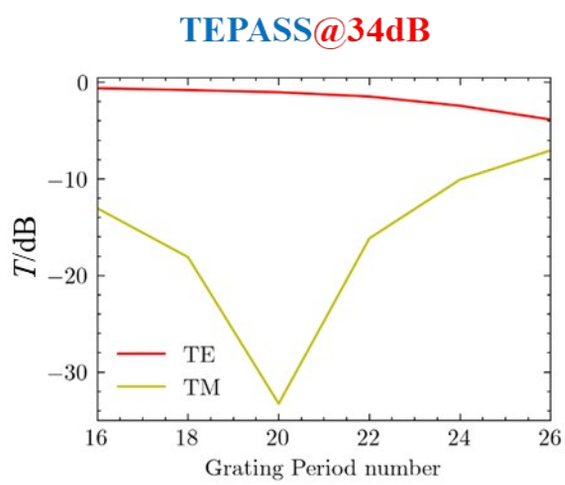

Fig. 5 Subwavelength grating TEPASS loss diagram
图5 亚波长光栅TEPASS损耗图

Table 1 Parameter tables for Subwavelength grating TEPASS
表1 亚波长光栅TEPASS的参数

Extinction polarization state	TEPASS
L_1(μm)	1
L_2(μm)	6
L_3(μm)	5
w_1(μm)	1
w_2(μm)	2
w_3(μm)	0.3
Λ(nm)	456
a(nm)	364.8

2 Fabrication and measurement

For device fabrication, we utilized 400 nm-thick lithium niobate thin films obtained from NANOLN, complemented by a silica layer of 4.7μm thickness. The fabrication process for the biconical coupling structures involved intricate steps, including two rounds of electron beam lithography (EBL) and two cycles of inductively coupled plasma reactive-ion etching (ICP-RIE). The

ICP-RIE was conducted at powers of 600 W for the source and 100 W for the bias, using pure argon as the etching gas, successfully achieving a ridge angle of 65°. The diagram below illustrates the Polarization Extinction Ratio (PER) testing system. The light source enters the Subwavelength Grating (SWG) chip via a grating coupling structure. PER measurements are conducted using the Santec PEM-340 equipment from Japan. During these tests, we use single-mode SMF28 optical fibers. We determine the PER values by measuring the polarization extinction ratios before and after the light enters the chip. The method for calculating the chip's polarization extinction ratio is outlined below:

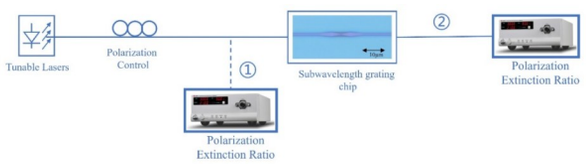

Fig. 6　Polarization extinction ratio test system
图6　偏振消光比测试系统

$$PER = PER_{out} - PER_{in} \quad , \quad (4)$$

After configuring this system for testing, the polarization extinction ratio (PER) of the waveguide was measured at 15 dB. The test data for the TEPASS subwavelength grating (SWG) are presented in Fig. 7. After calculations, we determined that the polarization extinction ratio for TEPASS at 1 550 nm was 29 dB. This performance exceeds that of polarization controllers described in existing literature, which are based on lithium niobate thin film devices.

It can be observed from Fig. 8 that TEPASS reaches a peak at a wavelength of 1 550 nm. The appearance of this peak is primarily due to the lack of calibration of the tunable laser's light source post-measurement, resulting in decreased stability of the output wavelength and power. Additionally, light of various wavelengths may encounter different levels of polarization mode dispersion

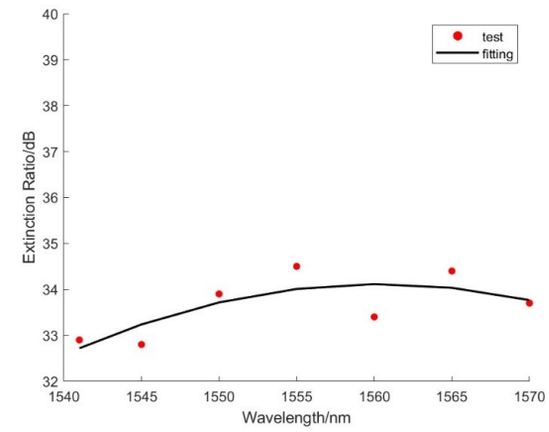

Fig. 7　TEPASS subwavelength grating test data
图7　亚波长光栅 TEPASS 测试数据

(PMD) and polarization-dependent loss (PDL) during testing.

Furthermore, Table 2 provides a comparison of different approaches to achieving polarization extinction ratios in lithium niobate thin films (LNOI), as reported in various studies. The table shows that this paper has achieved a polarization extinction ratio of 29 dB, the highest value reported to date. This result not only demonstrates the feasibility of achieving high polarization extinction ratios on a lithium niobate thin film platform, but also provides crucial reference solutions for future optical fiber sensing research.

3　Conclusion

This study presents a subwavelength grating (SWG) structure, designed using lithium niobate thin films. It focuses on the key performance metric of the polarization extinction ratio (PER), in Lithium Niobate on Insulator (LNOI). Experimental results demonstrate a remarkable PER of 29 dB at a wavelength of 1 550 nm. The successful application of this solution signifies major progress in utilizing lithium niobate thin films for fiber optic gyro-

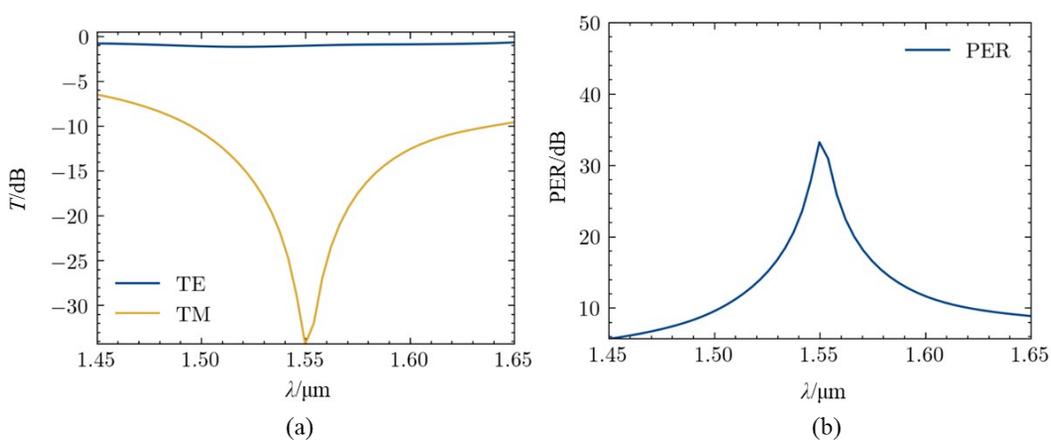

Fig. 8　(a) TE and TM loss diagrams at different wavelengths; (b) TEPASS polarization extinction ratio relationship diagram at different wavelengths
图8　(a) 不同波长下 TE 和 TM 损耗图; (b) 不同波长下 TEPASS 的偏振消光比关系图

Table 2 Comparison of PER solutions implemented on LNOI platform
表2 LNOI平台实现偏振消光方案对比

	PER@1 550 nm	result	size/μm	Extinction polarization state	IL@1 550 nm /dB
[7]	20	Simulated	23	TM	2
[6]	28.72	Simulated	1 000	TE	0.286
[6]	24.03	Simulated	1 000	TM	0.013
[2]	30.6	Experimental	55	TM	1.3
[3]	≈20	Experimental	300	TM	≈2
[3]	≈20	Experimental	300	TE	≈2
This work	29	Experimental	19.21	TE	1.5

scopes. It offers vital insights for future improvements in polarization splitting, extinction, and integrated optics. By optimizing LNOI's PER parameters, we expand the usage of lithium niobate thin films and offer useful guidance for the design and refinement of optical devices.

References

[1] Poberaj G, Hu H, Sohler W, *et al*. Lithium niobate on insulator (LNOI) for micro-photonic devices [J]. *Laser & Photonics Reviews*, 2012, **6**(4): 488-503.

[2] Han X, Chen L, Jiang Y, *et al*. Integrated Subwavelength Gratings on a Lithium Niobate on Insulator Platform for Mode and Polarization Manipulation [J]. *Laser & Photonics Reviews*, 2022, **16**(7): 2200130.

[3] Jin W, Chiang K S. Leaky-mode long-period grating on a lithium-niobate-on-insulator waveguide [J]. *Optica*, 2021, **8**(12): 1624-1631.

[4] LIU H-F, GUO H-J, TAN M-Q, *et al*. Research progress of lithium niobate thin-film modulators [J]. Chinese Optics, 2022, **15**(1): 1-13(刘海锋, 郭宏杰, 谭满清, 等. 铌酸锂薄膜调制器的研究进展 [J]. **中国光学(中英文)**), 2022, **15**(1): 1-13.

[5] Liu J-M, Zhang D-L. Ultra-broadband thin-film lithium niobate TM-pass waveguide polarizer using subwavelength grating metamaterial [J]. *Optics & Laser Technology*, 2023, **164**: 109556.

[6] Liu Y, Huang X, Li Z, *et al*. TE/TM-pass polarizers based on lateral leakage in a thin film lithium niobate – silicon nitride hybrid platform [J]. *Optics Letters*, 2020, **45**(17): 4915-4918.

[7] Yu W, Dai S, Zhao Q, *et al*. Wideband and compact TM-pass polarizer based on hybrid plasmonic grating in LNOI [J]. *Optics Express*, 2019, **27**(24): 34857-34863.

[8] Zhang D-L, Liu J-M. Air-Slot Assisted Tm-Pass Waveguide Polarizer Based on Lithium Niobate on Insulator [J]. *SSRN Electronic Journal*, 2022, 155: 108421.

[9] Luo Q, Bo F, Kong Y, *et al*. Advances in lithium niobate thin-film lasers and amplifiers: a review [J]. *Advanced Photonics*, 2023, **5**(3): 034002.

[10] Xu M, He M, Zhang H, *et al*. High-performance coherent optical modulators based on thin-film lithium niobate platform [J]. *Nature Communications*, 2020, **11**(1): 3911.

[11] Tao Z, Wang X. High extinction ratio, *low loss and broadband on-chip TE-pass polarizer for optical gyroscope*, 2022, 12283: 10-16,

[12] Guo H, Liu H, Lei M, *et al*. Research progress of integrated optical gyroscope [J]. *Chinese Optics Letters*, 2024, **22**(3): 031302.

[13] Han H, Xiang B. Integrated electro-optic modulators in x-cut lithium niobate thin film [J]. *Optik*, 2020, **212**: 164691.

[14] Zhu D, Shao L, Yu M, *et al*. Integrated photonics on thin-film lithium niobate [J]. *Advances in Optics and Photonics*, 2021, **13**(2): 242-352.

[15] Han X, Jiang Y, Xiao H, *et al*. Subwavelength Grating-Assisted Contra-Directional Couplers in Lithium Niobate on Insulator [J]. *Laser & Photonics Reviews*, 2023, **17**(10): 2300203.

[16] Weigel P O, Zhao J, Fang K, *et al*. Bonded thin film lithium niobate modulator on a silicon photonics platform exceeding 100 GHz 3-dB electrical modulation bandwidth [J]. *Optics Express*, 2018, **26**(18): 23728-23739.

[17] Guo H J, Liu H F, Wang Z N, *et al*. Design of a novel Y-junction electro-optic modulator based on thin film lithium niobite [J]. *Journal of Infrared and Millimeter Waves*, **41**(3): 626-630.